

NANOFLUID FLOW ON A VERTICAL CYLINDER UNDER THE EFFECT OF MAGNETOHYDRODYNAMICS

Asst. Prof. Dr. Manal H. Saleh
University of Baghdad/ college of Engineering
Mechanical Dept

Manalhadi2005@yahoo.com

ABSTRACT

The present work is a numerical investigation of the effect of laminar natural convection flow of nano fluid taking Cu nano particles and the water as based fluid on a vertical cylinder in presence of magneto hydrodynamics. The governing equations which used are continuity, momentum and energy equations. These equations are transformed to dimensionless equations using vorticity-stream function method and the resulting nonlinear system of partial differential equations are then solved numerically using finite difference approximation. A thermal boundary condition of a constant wall temperature is considered. A computer program was built to calculate the rate of heat transfer in terms of average Nusselt number, velocity distribution as well as temperature distribution for magneto hydrodynamics range of $(0.0 \leq M \leq 100)$ and the volume fraction $(0 \leq \varphi \leq 0.4)$. Numerical solution have been considered for a fluid Prandtl number fixed at $(Pr = 6.2)$, Rayleigh number $(10^2 \leq Ra_l \leq 10^4)$. The results show that Nu increase with increasing Ra_l and M and increased with the particle volume fraction up to $\varphi = 0.15$ then decreased due to viscosity and agglomeration effect. The effect of Rayleigh number and magneto hydrodynamics on the rate of heat transfer is concluded by a correlation equation.

KEY WORDS: natural convection, nanofluid, magneto hydrodynamics, vertical cylinder

جريان مائع نانوي على سطح أسطوانة عمودية تحت تأثير المغناطيسية
الهيدروديناميكية

أ.م.د. منال هادي صالح
جامعة بغداد/ كلية الهندسة/ قسم الهندسة الميكانيكية

الخلاصة:

تمت دراسة عددية لبيان تأثير الحمل الحر لجريان طبقي لمائع النانو باستخدام جسيمات النحاس Cu الدقيقة والماء كمائع أساس على اسطوانة عمودية تحت تأثير المغناطيسية الهيدروديناميكية . المعادلات الحاكمة هي الاستمرارية والزخم ومعادلة الطاقة وتم تحويلها الى معادلات لا بعدية باستخدام دالة الانسياب الدوامية وتم حل

المعادلات التفاضلية الجزئية عدديا باستخدام طريقة الفروق المحددة والظروف الحدية الحرارية التي أخذت بنظر الاعتبار هي ثبوت درجة حرارة الجدار. تم بناء برنامج حاسوبي لحساب معدل انتقال الطاقة الحرارية بدلالة عدد نسلت المعدل وتوزيع السرعة ودرجة الحرارة للمعايير التي تتضمن مجموعة من القيم اللابعديّة كالمغناطيسية الهيدروديناميكية اللابعديّة ($0.0 \leq M \leq 100$) ونسب حجم الجسيمات المضافة ($0 \leq \phi \leq 0.4$). اخذ بنظر الاعتبار الحل العددي لمائع ذو عدد براندتل ($Pr=6.2$) وعدد رايلي ($10^2 \leq Ra_l \leq 10^4$). النتائج بينت أن عدد نسلت يزداد بزيادة عدد رايلي Ra_l والمغناطيسية الهيدروديناميكية M وبزيادة نسب حجم الجسيمات حتى تصل إلى $\phi=0.15$ ثم يبدأ عدد نسلت بالنقصان بسبب تأثير اللزوجة والتراكمات. تم تمثيل النتائج بمعادلة ترابطية لعدد نسلت ضد عدد رايلي والمغناطيسية الهيدروديناميكية.

INTRODUCTION

A liquid coolant is widely used to prevent the overheating or heat transfer rate improvement of equipments such as electronic devices, heat exchangers and transportation vehicles. However, conventional heat transfer fluid such as water or ethylene glycol generally has poor thermal properties. So, many efforts for dispersing small particles with high thermal conductivity in the liquid coolant have been conducted to enhance thermal properties of the conventional heat transfer fluids. The early research, which used suspension and dispersion of millimeter- and micrometer- sized particles, faced the major problem of poor suspension stability. Thus, a new class of fluid for improving both thermal conductivity and suspension stability is required in the various industrial fields. This motivation leads to development of nanofluids. Nanofluid is a new kind of fluid consisting of uniformly dispersed and suspended nanometer-sized particles or fibers in fluids and has unprecedented thermal characteristics [Kyo et al., 2009].

A numerical study has been conducted by [Grosan and Pop, 2011] to investigate the steady axisymmetric mixed convection boundary layer flow past a thin vertical cylinder placed in a water-based copper (Cu) nanofluid. Numerical results are obtained for the skin-friction coefficient and Nusselt number as well as for the velocity and temperature profiles for some values of the governing parameters, namely, the nanoparticles volume fraction parameter ϕ , mixed convection parameter k and the curvature parameter c with the Prandtl number $Pr = 6.2$ (water). The results indicate that dual solutions exist when the surface of the cylinder is cooled (opposing flow, $k < 0$). [Mohammad and Ariyan, 2011] Investigated numerically the flow-field and heat transfer through a copper-water nanofluid around circular cylinder. Reynolds and Peclet numbers (based on the cylinder diameter and the velocity of free stream) are within the range of 1 to 40. Furthermore, volume fraction of nanoparticles (ϕ) varies within the range of 0 to 0.05. It is found that the vorticity, pressure coefficient, recirculation length are increased by the addition of nanoparticles into clear fluid. Moreover, the local and mean Nusselt numbers are enhanced due to adding nanoparticles into base fluid. [Nazar et al., 2011] Studied Steady mixed convection boundary layer flow from an isothermal horizontal circular cylinder embedded in a porous medium filled with a nanofluid for both cases of a heated and cooled cylinder. Three different types of nanoparticles are considered, namely Cu, TiO_2 and Al_2O_3 . It is found that when fraction ϕ increases, the magnitude of the skin friction coefficient decreases, and this leads to an increase in the value of the mixed convection parameter λ which first produces no separation. On the other hand, it is also found that of all the three types of nanoparticles considered, for any fixed values of ϕ and λ , the



nanoparticle Cu gives the largest values of the skin friction coefficient followed by TiO₂ and Al₂O₃. Finally, it is worth mentioning that heating the cylinder ($\lambda > 0$) delays separation of the boundary layer and if the cylinder is hot enough (large values of $\lambda > 0$), then it is suppressed completely. On the other hand, cooling the cylinder ($\lambda < 0$) brings the boundary layer separation point nearer to the lower stagnation point and for a sufficiently cold cylinder (large values of $\lambda < 0$) there will not be a boundary layer on the cylinder. [Sheikholeslami et al., 2012], Investigated numerically natural convection in a concentric annulus between a cold outer square and heated inner circular cylinders in presence of static radial magnetic field using the lattice Boltzmann method. The effective thermal conductivity and viscosity of nanofluids are calculated using the Maxwell–Garnetts (MG) and Brinkman models, respectively. The results reveal that the average Nusselt number is an increasing function of nanoparticle volume fraction as well as the Rayleigh number, while it is a decreasing function of the Hartmann number. [Mina et al., 2011] Studied numerically laminar conjugate heat transfer by natural convection and conduction in a vertical annulus formed between an inner heat generating solid circular cylinder and an outer isothermal cylindrical boundary. It is assumed that the two sealed ends of the tube to be adiabatic. Results are presented for the flow and temperature distributions and Nusselt numbers on different cross sectional planes and longitudinal sections for Rayleigh number ranging from 10^5 to 10^8 , solid volume fraction of $0 < \phi < 0.05$ with copper-water nanofluid as the working medium. Considering that the driven flow in the annular tube is strongly influenced by orientation of tube, study has been carried out for different inclination angles.

In the present study, the magneto hydrodynamic, effect was investigated for steady state laminar natural convection external flow of nano fluids on a vertical cylinder, for thermal boundary condition of constant wall temperature at all walls and for ($10^2 \leq Ra_1 \leq 10^4$), ($0 \leq M \leq 100$) and ($0 \leq \phi \leq 0.4$).

MATHEMATICAL MODEL

The mathematical modeling will be set for laminar natural convection heat transfer of nanofluid on a vertical cylinder. The buoyancy effect caused by the density variation produces natural circulation resulting in the fluid motion relative to the bounding solid surface. The buoyancy forces behave as body forces and are included as such in the momentum equation. Under these conditions the continuity, momentum and energy equations are coupled.

The effective thermal conductivity of the nano-fluid is approximated by Maxwell-Garnetts model:

$$\frac{k_{nf}}{k_f} = \frac{k_s + 2k_f - 2\phi(k_f - k_s)}{k_s + 2k_f + \phi(k_f - k_s)} \quad (1)$$

The use of this equation is restricted to spherical nano-particles where it dose not account for other shapes of nano-particles. This model is found to be appropriate for studying heat transfer enhancement using nanofluid [Akbrinia and Behzadmehr, 2007] and [Eiyad, 2008]. The viscosity of the nano-fluid can be approximated as viscosity of a base fluid μ_f containing dilute suspension of fine spherical particles and is given by [Khanafar et al., 2003]:



$$\mu_{nf} = \frac{\mu_f}{(1-\phi)^{2.5}} \quad (2)$$

The effective density of the nanofluid is given as:

$$\rho_{nf} = \phi \rho_s + (1-\phi) \rho_f \quad (3)$$

The heat capacitance of the nano-fluid is expressed as [Eiyad, 2008] and [Khanafar et al., 2003]:

$$(\rho \cdot C_p)_{nf} = \phi (\rho \cdot C_p)_s + (1-\phi) (\rho \cdot C_p)_f \quad (4)$$

The thermo physical properties of water and copper at 300 K are given in **Table (1)**.

Continuity Equation

The equation of conservation of mass in the cylindrical coordinates is given as:

$$\frac{1}{r} \frac{\partial}{\partial r} (r u) + \frac{\partial w}{\partial z} = 0 \quad (5)$$

Momentum Equation

By using Navier-Stokes' equation in the cylindrical coordinates (r, z), the equation of conservation of momentum in the cylindrical coordinates (the radial (r) direction) is in the following form:

$$u \frac{\partial u}{\partial r} + w \frac{\partial u}{\partial z} = -\frac{1}{\rho_{nf}} \frac{\partial P^*}{\partial r} + \frac{\mu_{nf}}{\rho_{nf}} \left(\frac{\partial}{\partial r} \left[\frac{1}{r} \frac{\partial}{\partial r} (r u) \right] + \frac{\partial^2 u}{\partial z^2} \right) + f_r \quad (6)$$

Where (f_r) is the electromagnetic force in (r) direction [Herman, 1978]

$$f_r = \frac{\sigma_o B_o^2 u}{\rho}$$

The equation of conservation of momentum in the cylindrical coordinates (in the axial (z) direction) is in the following form:

$$u \frac{\partial w}{\partial r} + w \frac{\partial w}{\partial z} = -\frac{1}{\rho_{nf}} \frac{\partial P^*}{\partial z} + \frac{\mu_{nf}}{\rho_{nf}} \left(\frac{1}{r} \frac{\partial}{\partial r} \left[r \frac{\partial w}{\partial r} \right] + \frac{\partial^2 w}{\partial z^2} \right) + C_1 g (T - T_\infty) + f_z \quad (7)$$



$$\text{Where } C_1 = \frac{\phi \rho_s \beta_s + (1-\phi) \rho_f \beta_f}{\rho_{nf}}$$

(f_z) is the electromagnetic force in (z) direction [Herman, 1978].

$$f_z = \frac{\sigma_o B_o^2 w}{\rho}$$

Energy Equation

The energy equation in the cylindrical coordinates takes the following form:

$$u \frac{\partial T}{\partial r} + w \frac{\partial T}{\partial z} = \alpha_{nf} \left(\frac{1}{r} \frac{\partial}{\partial r} \left[r \frac{\partial T}{\partial r} \right] + \frac{\partial^2 T}{\partial z^2} \right) \quad (8)$$

$$\alpha_{nf} = \frac{k_{nf}}{(\rho \cdot C_p)_{nf}}$$

DIMENSIONLESS PARAMETERS AND EQUATIONS

$$\left(R = \frac{r}{l} \right), \quad \left(Z = \frac{z}{l} \right), \quad \left(U = \frac{u a}{\alpha_{nf}} \right), \quad \left(W = \frac{w a}{\alpha_{nf}} \right), \quad \left(\theta = \frac{T - T_\infty}{T_w - T_\infty} \right),$$

$$\left(P = \frac{P^* l^2}{\rho \alpha_{nf}^2} \right), \quad \left(M = \frac{\sigma_o B_o^2 l^2}{\rho \alpha_{nf}} \right)$$

Dimensionless Continuity Equation

$$\frac{1}{R} \frac{\partial(RU)}{\partial R} + \frac{\partial W}{\partial Z} = 0 \quad (9)$$

Dimensionless Momentum Equation In (r) Direction

$$U \frac{\partial U}{\partial R} + W \frac{\partial U}{\partial Z} = -\frac{\partial P}{\partial R} + C_2 \left(\frac{\partial}{\partial R} \left(\frac{1}{R} \frac{\partial(RU)}{\partial R} \right) + \frac{\partial^2 W}{\partial Z^2} \right) + MU \quad (10)$$

Dimensionless Momentum Equation In (z) Direction

$$U \frac{\partial W}{\partial R} + W \frac{\partial W}{\partial Z} = -\frac{\partial P}{\partial Z} + C_2 \left(\frac{1}{R} \frac{\partial}{\partial R} \left(R \frac{\partial W}{\partial R} \right) + \frac{\partial^2 W}{\partial Z^2} \right) + C_3 \cdot \theta + MW \quad (11)$$



Where:

$$C_2 = \frac{\text{Pr}}{(1-\phi)^{0.25} \cdot \left[(1-\phi) + \phi \frac{\rho_s}{\rho_f} \right]}$$

$$C_3 = Ra_l \cdot \text{Pr} \left[\frac{1}{\frac{(1-\phi) \rho_f}{\phi \rho_s} + 1} \frac{\beta_s}{\beta_f} + \frac{1}{\frac{\phi \rho_f}{(1-\phi) \rho_s} + 1} \right]$$

Dimensionless Energy Equation

$$U \frac{\partial \theta}{\partial R} + W \frac{\partial \theta}{\partial Z} = \left[\frac{1}{R} \frac{\partial}{\partial R} (\lambda R \frac{\partial \theta}{\partial R}) \right] + \lambda \frac{\partial^2 \theta}{\partial Z^2} \quad (12)$$

$$\lambda = \frac{k_{nf}/k_f}{(1-\phi) + \phi \frac{(\rho \cdot C_p)_s}{(\rho \cdot C_p)_f}}$$

Vorticity Transport, Stream Function and Energy Equation

The governing equations in dimensionless form above were written in terms of dependant variables (U , W , P and θ). It may be recommended to eliminate pressure term (because it will be a non linear term in momentum equation)[Patanker, 1980]. By converting momentum equations to vorticity transport equation by differentiate momentum equation in (r) direction with respect to (z) and momentum equation in (z) direction with respect to (r) and subtract them from each other and make use of continuity equation and vorticity definition:

$$\omega = \frac{\partial W}{\partial R} - \frac{\partial U}{\partial Z} \quad (13)$$

$$\frac{\partial(U\omega)}{\partial R} + \frac{\partial(W\omega)}{\partial Z} = C_2 \left(\frac{\partial}{\partial R} \left(\frac{1}{R} \frac{\partial(R\omega)}{\partial R} \right) + \frac{\partial^2 \omega}{\partial Z^2} \right) + C_3 \frac{\partial \theta}{\partial R} + M\omega \quad (14)$$

Also, by making use of vorticity definition (13) and the definition of stream function, (ψ) which satisfy continuity equation, the vertical and radial velocities can be written as follows respectively:

$$W = -\frac{1}{R} \frac{\partial \psi}{\partial R} \quad (15)$$



$$U = \frac{1}{R} \frac{\partial \psi}{\partial Z} \quad (16)$$

So by substituting the velocity components (15) and (16) in vorticity definition equation (13), stream function equation resulted as:

$$-\omega = \frac{1}{R} \left(\frac{\partial^2 \psi}{\partial R^2} - \frac{1}{R} \frac{\partial \psi}{\partial R} + \frac{\partial^2 \psi}{\partial Z^2} \right) = \nabla^2 \psi \quad (17)$$

The dimensionless energy equation (12) can be transformed to another form by substituting the continuity equation (9) in it as follows:

$$\frac{1}{R} \frac{\partial (RU\theta)}{\partial R} + \frac{\partial (W\theta)}{\partial Z} = \left[\frac{1}{R} \frac{\partial}{\partial R} \left(\lambda R \frac{\partial \theta}{\partial R} \right) \right] + \lambda \frac{\partial^2 \theta}{\partial Z^2} \quad (18)$$

Boundary Conditions;

The imposed boundary conditions (illustrate in **Fig. (1)** and **Table (2)**), rewritten in terms of stream function and vorticity

$$\omega = \psi = U = W = 0 \text{ (No slip condition)}$$

$$\theta = 1 \quad \text{(Constant wall temperatures)}$$

NUMERICAL SOLUTION

The method of the numerical solution taken is the Finite Difference technique for solving the set of equations:

$$a_1 \theta_{i-1,j} + a_2 \theta_{i+1,j} + a_3 \theta_{i,j} + a_4 \theta_{i,j-1} + a_5 \theta_{i,j+1} = 0 \quad (19)$$

Where:

$$a_1 = \frac{(U_b + |U_b|)(\Delta R(1-2i) - R_i)}{4\Delta R(R_i + i\Delta R)} + \left(-\frac{\lambda}{(\Delta R)^2} + \frac{\lambda}{2\Delta R(R_i + \Delta R)} \right) \quad (20)$$

$$a_2 = \frac{(U_f - |U_f|)(R_i + \Delta R(1+2i))}{4\Delta R(R_i + i\Delta R)} - \left(\frac{\lambda}{\Delta R^2} + \frac{\lambda}{2\Delta R(R_i + \Delta R)} \right) \quad (21)$$



$$a_3 = \frac{[(U_f + |U_f|)(R_i + \Delta R(1 + 2i)) + (U_b - |U_b|)(\Delta R(1 - 2i) - R_i)]}{4\Delta R(R_i + i\Delta R)} + \frac{(W_f + |W_f| - W_b + |W_b|)}{2\Delta Z} + \frac{2}{(\Delta R)^2} + \frac{2}{(\Delta Z)^2} \quad (22)$$

$$a_4 = \frac{(-W_b + |W_b|)}{2\Delta Z} - \frac{1}{(\Delta Z)^2} \quad (23)$$

$$a_5 = \frac{(W_f - |W_f|)}{2\Delta Z} - \frac{1}{(\Delta Z)^2} \quad (24)$$

$$b_1\omega_{i-1,j} + b_2\omega_{i+1,j} + b_3\omega_{i,j} + b_4\omega_{i,j-1} + b_5\omega_{i,j+1} + c = 0 \quad (25)$$

Where:

$$b_1 = -\frac{(U_b + |U_b|)}{2\Delta R} + \frac{1}{2\Delta R(R_i + i\Delta R)} - \frac{1}{(\Delta R)^2} \quad (26)$$

$$b_2 = \frac{(|U_f| - U_f)}{2\Delta R} - \frac{1}{2\Delta R(R_i + i\Delta R)} - \frac{1}{(\Delta R)^2} \quad (27)$$

$$b_3 = -M + \frac{[(U_f + |U_f|) - (U_b + |U_b|)]}{2\Delta R} + \frac{(W_f + |W_f| - W_b + |W_b|)}{2\Delta Z} + \frac{2C_2}{(\Delta R)^2} + \frac{2C_2}{(\Delta Z)^2} + \frac{C_2}{(R_i + i\Delta R)^2} \quad (28)$$

$$b_4 = -\frac{(W_b + |W_b|)}{2\Delta Z} - \frac{C_2}{(\Delta Z)^2} \quad (29)$$

$$b_5 = \frac{(W_f - |W_f|)}{2\Delta Z} + \frac{C_2}{(\Delta Z)^2} \quad (30)$$

$$c = -\frac{C_3(\theta_{i+1,j} - \theta_{i-1,j})}{2\Delta R} \quad (31)$$



$$\psi_{i,j}^{it+1} = (1-\Omega) \psi_{i,j}^{it} + \frac{\Omega}{4} \left[\begin{aligned} & (R_i + i\Delta R)(\Delta R)^2 \omega'_{i,j} + \left(\frac{R_i + \Delta R(i-0.5)}{(R_i + i\Delta R)} \right) \psi_{i+1,j}^{it} \\ & \left(\frac{R_i + \Delta R(i+0.5)}{(R_i + i\Delta R)} \right) \psi_{i-1,j}^{it+1} + (\psi_{i,j+1}^{it+1} + \psi_{i,j-1}^{it+1}) \end{aligned} \right] \quad (32)$$

Where the parameter (Ω) is the over relaxation coefficient and its value is ($1 \leq \Omega \leq 1.5$). The local Nusselt number at the heated wall:

$$Nu_l = -\frac{k_{nf}}{k_f} \left(\frac{\partial \theta}{\partial R} \right) \quad (33)$$

The average Nusselt number along a single channel wall is defined by [Schwab and De Witt, 1970]:

$$Nu = -\frac{1}{l} \int_0^l Nu_l dZ \quad (34)$$

RESULTS AND DISCUSION

Finite difference solution for laminar natural convection flow of a water based nanofluids on a vertical cylinder in presence of magnetohydrodynamics was presented.

Effect of Different Parameters on Heat Transfer:

Streamlines and Isotherms:

Fig.(2) shows the streamlines and isotherms for $\phi=0$, $Ra_1 = 10^2$ with no magneto hydrodynamic (MHD). The mechanism of the flow occurs when the fluid near the hot wall is heated causing the density to be decreased and the fluid will be start to move upward nearby the hot wall towards the cold wall. It can be seen that the values of streamlines and isotherms at the cylinder surface increased when Ra_1 increased in **Fig. (3)**. The isotherms will be closer to the cylinder and its value decreased from the surface to the ambient as Ra_1 increased.

Fig. (4) and **Fig.(5)** show the effect of MHD for different values of Ra_1 and with $\phi=0$. It is clear that the increase of MHD cause to increase in the values of streamlines and a wide region of temperature distribution in the lateral direction for $Ra_1(10^2)$ but for higher Ra_1 the region of temperature distribution will be decreased and the streamlines will be closer to the cylinder. It is interesting to note that as the strength of the magnetic field increases the central streamlines are elongated horizontally and the temperature stratification in the core diminishes. The isotherms are almost parallel and are nearly conduction like and this is due to the suppression of convection by the magnetic field. For higher Rayleigh number and low MHD, the thermal boundary layers are well established along the side walls and the temperature stratification exists. This is because convection is the dominant mode of heat transfer at high Rayleigh number. From these figures, it is also observed that for higher Rayleigh number the effect of MHD on the temperature distribution is not prominent compared to that in the case of small Ra_1 .



A distinct increase in streamlines and isotherms are shown in **Fig. (6)** and **Fig. (7)** for $\phi=0.4$ compared with that in **Fig.(2)** and **Fig. (3)** for $\phi=0$. The flow exhibits a simple circulating pattern rising a long the hot wall and descending along the cold wall of the cylinder.

The Variation of average Nu with Ra_1 :

Fig. (8) Presents the variation of average Nusselt number with volume fraction for different values of Rayleigh number and M. The figure shows that the heat transfer increases almost monotonically with increasing the volume fraction for all Rayleigh numbers and M. As volume fraction of nanoparticles increases, difference for average Nusselt number becomes larger especially at higher Rayleigh numbers due to increasing of domination of convection mode of heat transfer. Effect of nanoparticles on enhancement of heat transfer at low Rayleigh numbers is more significant than that at high Rayleigh numbers. This behavior is true for all considered values of M. The decreasing trend in the normalized average Nusselt number as ϕ increases is associated to the Maxwell-Garnetts model meaning that the effect of the thermal conductivity models is less significant than the viscosity models at high Rayleigh number and due to agglomeration of particles. For low Rayleigh number, the same enhancement features in the average Nusselt number as ϕ increases are predicted upon using the Maxwell-Garnetts model. The best value of ϕ is 0.15% for all the values of Ra_1 and M. the variation of average Nusselt number with Rayleigh number illustrated in **Fig (9)** for different values of ϕ which show the best effect at Ra_1 equal about 500.

The Effect of MHD on Nu Including Other Parameters:

Fig.(10) shows the variation of Nu with ϕ for different values of M and Rayleigh number = 10^4 . It is clear that at low values of M the effect is very low and the curves consolidate but for large values of M the increase in average Nu is significant, for example at $\phi =0.15\%$ and $M=100$, the increase in Nu =20.5% and **Fig. (11)** shows that for $M > 10$, the effect of MHD is more significant.

A correlation has been set up to give the average Nusselt number variation with Ra_1 , M and. This correlation is made by using the computer program (DGA v1.00).

$$Nu = 1.963Ra_1^{0.951}M^{0.837}$$

CONCLUSIONS

From the present work results and for the cylinder that described previously, the following conclusions can be obtained:

1. The average Nusselt number (Nu) increases by 88.8% with the increase of Rayleigh number (Ra_1) from 10^2 to 10^4 for $\phi=0.1$ and $M=0$.
2. The average Nusselt number Nu increases by 20.5 % with increase MHD parameter M from 0 to 100 for $\phi=0.15$ and $Ra_1 =10^4$.
3. The decreasing trend in the normalized average Nusselt number as ϕ increases is associated to the Maxwell-Garnetts model meaning that the effect of the thermal conductivity models is less significant than the viscosity models at high Rayleigh number.



REFERENCES

- [1] KyoSik Hwang, SeokPil Jang, Stephen U.S. Choi, " Flow and convective heat transfer characteristics of water-based Al_2O_3 nanofluids in fully developed laminar flow regime", International Journal of Heat and Mass Transfer 52 (2009) 193–199.
- [2] Mohammad SadeghValipour ,AriyanZareGhadi " Numerical investigation of fluid flow and heat transfer around a solid circular cylinder utilizing nanofluid", International Communications in Heat and Mass Transfer 38 (2011) 1296–1304.
- [3] T. Grosan , I. Pop," Axisymmetric mixed convection boundary layer flow past a vertical cylinder in a nanofluid", International Journal of Heat and Mass Transfer 54 (2011) 3139–3145.
- [4] R. Nazar · L. Tham · I. Pop · D. B. Ingham," Mixed Convection Boundary Layer Flow from a Horizontal Circular Cylinder Embedded in a Porous Medium Filled with a Nanofluid", Transp Porous Med (2011) 86:517–536.
- [5] M. Sheikholeslami , M. Gorji-Bandpay, D.D. Ganji," Magnetic field effects on natural convection around a horizontal circular cylinder inside a square enclosure filled with nanofluid", International Communications in Heat and Mass Transfer 39 (2012) 978–986.
- [6] Mina Shahi, Amir HoushangMahmoudi , FarhadTalebi," A numerical investigation of conjugated-natural convection heat transfer enhancement of a nanofluid in an annular tube driven by inner heat generating solid cylinder", International Communications in Heat and Mass Transfer 38 (2011) 533–542.
- [7] Akbrinia A., Behzadmehr A.," Numerical Study of Laminar Mixed Convection of a Nanofluid in Horizontal Curved Tubes", Applied Thermal Eng., vol. 27,2007, pp. 1327-1337.
- [8] Eiyad A.N," Application of Nanofluids for Heat Transfer Enhancement of Separated Flows Encountered in a Backward Facing Step", Int. Journal of Heat and Fluid Flow, vol. 29, 2008, pp. 242-249.
- [9] Khanafer K., Vafai K., and Lightstone M., " Bouyancy-driven Heat Transfer Enhancement in a Two-Dimensional Enclosure Utilizing Nanofluids", Int. Journal Heat Mass Transfer, vol. 46, 2003, pp. 3639-3653.
- [10] Herman Branover, 1978"Magneto hydrodynamic Flow in Ducts" The MIT Cambridge, Massachusetts, and London, England.
- [11] Patanker, S. V., 1980 "Numerical Heat Transfer and Fluid Flow", Series in Computational Methods, McGraw-Hill, 1st Edition.
- [12] Schwab, T. H., and De Witt, K. J., 1970 "Numerical Investigation of Free Convection between Two Vertical Coaxial Cylinders", AIChE J., Vol. 16, PP.1005-1010.
- [13]Israa Y. Daood, "Effects of Nano-Fluids Types, Volume Fraction of Nano-Particles, and Aspect Ratios on Natural Convection Heat Transfer in Right- Angle Triangular Enclosure", Eng. And Tech. Journal, vol. 28, No. 16, 2010, pp. 5365-5388.

NOMENCLATUR

LATIN SYMBOLS

Symbol	Description	Unit
B_o	Strength of magnetic field	-
Cp_s, Cp_f, Cp_{nf}	Specific heat at constant pressure for solid, fluid and nanofluids respectively	kJ/kg.K
f_r	Electromagnetic force in (r) direction	m/s ²
f_z	Electromagnetic force in (z) direction	m/s ²
g	Acceleration due to gravity	m/s ²
k_s, k_f, k_{nf}	Thermal conductivity for solid, fluid and nanofluids respectively	W/m.°C
l	Length of cylinder	m
M	Dimensionless Magneto hydrodynamic parameter	-
Nu	Average Nusselt number($Nu=hl/k$)	-
P^*	Air pressure	N/m ²
P	Normalized air pressure	-
Pr	Prandtl number($Pr=v/\alpha$)	-
r	Radial direction	m
R	Dimensionless Radial direction	-
Ra_l	Rayleigh no. $\left(Ra_l = \frac{Pr g \beta (T_w - T_\infty) l^3}{\nu^2} \right)$	-
T	Air temperature	K
T_∞	Ambient temperature	K
u	Radial velocity	m/s
U	Dimensionless Radial velocity	-
w	Vertical velocity	m/s
W	Dimensionless Vertical velocity	-
z	Vertical direction	m
Z	Dimensionless Vertical direction	-

CREAK SYMBOLS:

Symbol	Description	Unit
α_{nf}	Thermal diffusivity of nanofluid	m ² /s
β_s, β_f	Coefficient of thermal expansion for solid and fluid respectively	K ⁻¹
θ	Dimensionless temperature	-
μ_s, μ_f, μ_{nf}	Dynamic viscosity for solid and fluid respectively	kg/m.s
$\rho_s, \rho_f, \rho_{nf}$	Density of solid, fluid and nanofluids respectively	kg/m ³
Ψ	Dimensionless stream function	-
ω	Dimensionless vorticity	-
φ	Volume fraction	-
σ_o	Electrical conductivity of the fluid	-

Subscript

Symbol	Description	Unit
(i,j)	Grid nodes in (r,z) direction	-

Table (1) Thermo Physical Properties of Fluid and Nanoparticles [Israa, 2010]

Physical properties	Cu	Water
C_p (J/kg K)	385	4179
ρ (kg/m ³)	8933	997.1
k (W/m K)	400	0.613
$\alpha \times 10^{-7}$ (m ² /s)	1163.1	1.47
$\beta \times 10^5$ (1/K)	1.67	21

Table (2) Boundary Conditions

Line	Θ	ψ	ω	W,U
AB	$\frac{\partial \theta}{\partial R} = 0$	0.0	0.0	0.0
BC	1.0	0.0	$\omega = -\frac{1}{Z} \frac{\partial^2 \psi}{\partial R^2}$	0.0
CD	1.0	0.0	$\omega = -\frac{1}{R} \frac{\partial^2 \psi}{\partial Z^2}$	0.0
DE	1.0	0.0	$\omega = -\frac{1}{Z} \frac{\partial^2 \psi}{\partial R^2}$	0.0
EF	$\frac{\partial \theta}{\partial R} = 0$	0.0	0.0	0.0
FG	0.0	$\frac{\partial \psi}{\partial Z} = 0$	0.0	0.0
GH	0.0	$\frac{\partial \psi}{\partial R} = 0$	0.0	0.0
HA	$\frac{\partial \theta}{\partial Z} = 0$	$\frac{\partial \psi}{\partial Z} = 0$	0.0	0.0

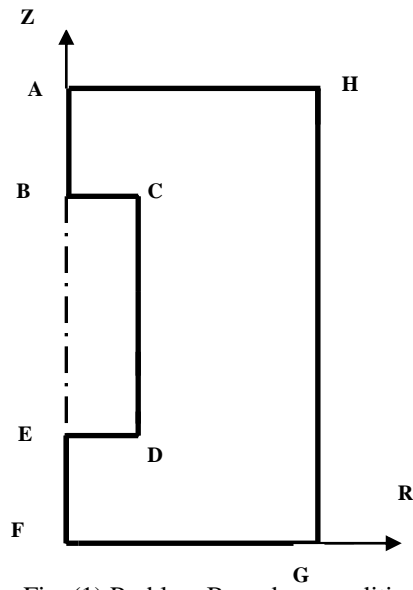


Fig. (1) Problem Boundary condition of the

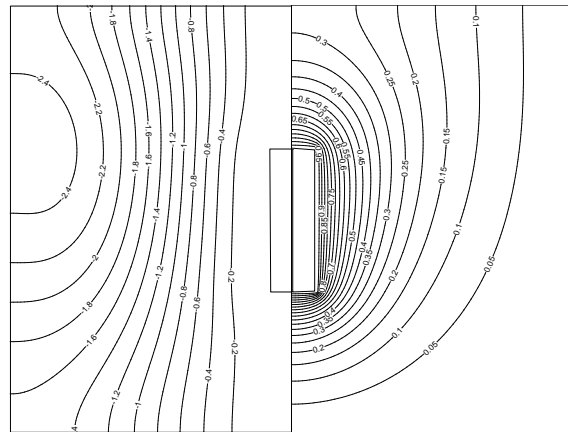


Fig. (2) Streamlines and isotherms for $M=0, \varphi=0$ at $Ra_1 = 10^2$

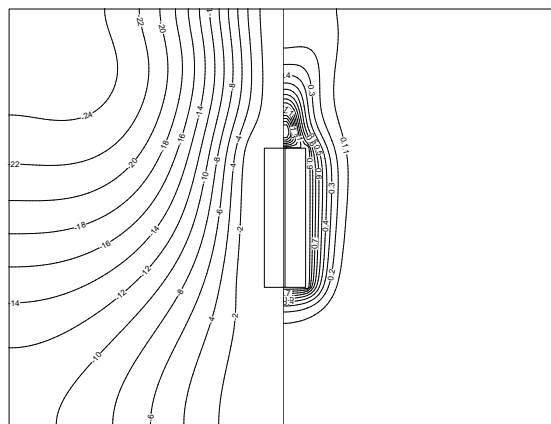


Fig. (3) Streamlines and isotherms for $M=0, \varphi=0$ at $Ra_1 = 10^4$

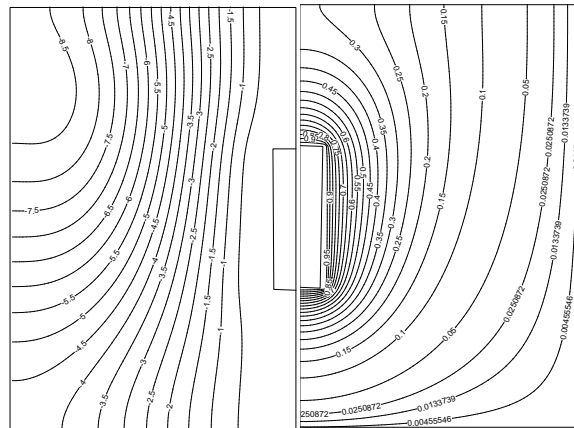


Fig. (4) Streamlines and isotherms for $M=100$, $\phi=0$ at $Ra_1=10^2$

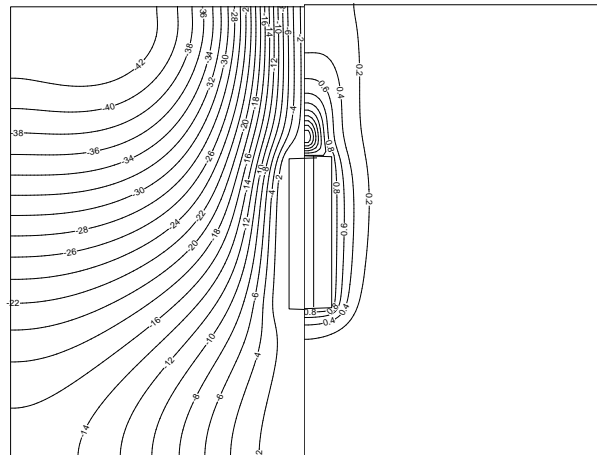


Fig. (5) Streamlines and isotherms for $M=100$, $\phi=0$ at $Ra_1=10^4$

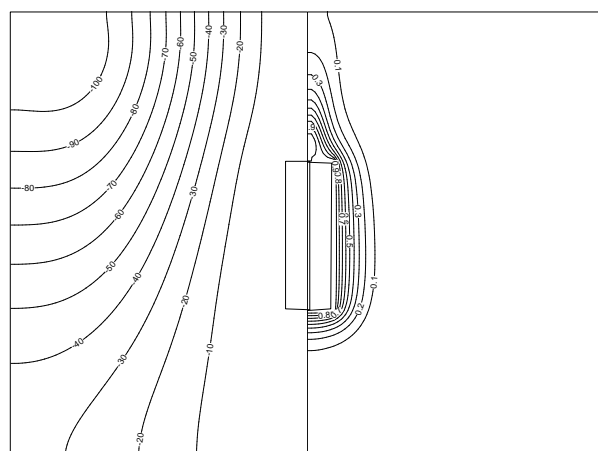


Fig. (6) Streamlines and isotherms for $M=0$, $\phi=0.2$ at $Ra_1=10^2$

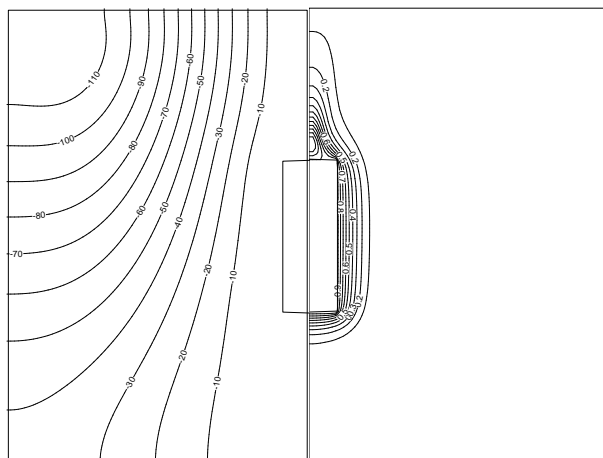


Fig. (7) Streamlines and isotherms for $M=0$, $\phi=0.2$ at $Ra_1 = 10^4$

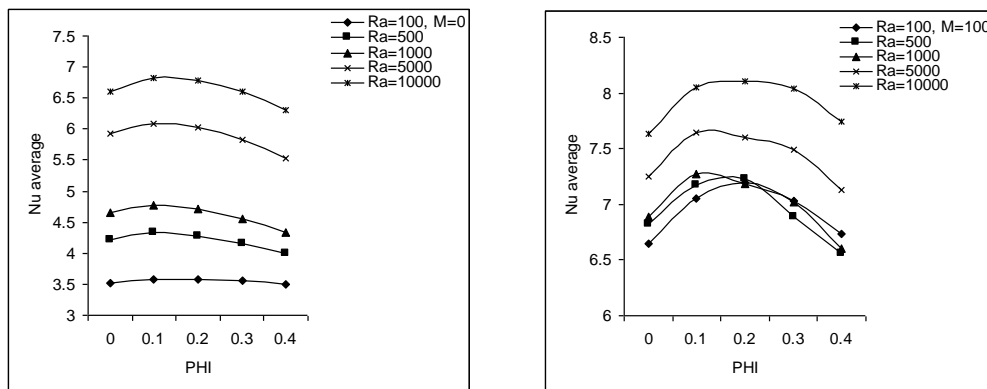


Fig. (8) Variation of average Nusselt number with volume fraction for $M=0$ and $M=100$ respectively and for different Rayleigh number

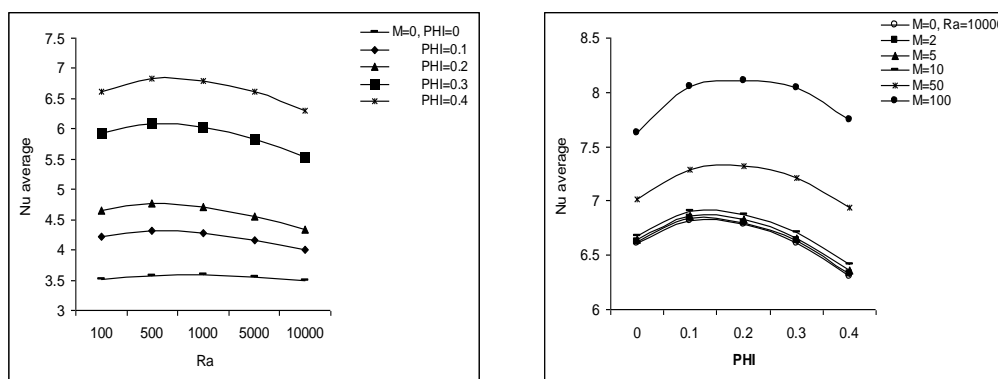


Fig. (9) Variation of average Nusselt number with Rayleigh number for $M=0$ and for different volume fraction for different M

Fig. (10) Variation of average Nusselt number with volume fraction for $Ra_1 = 10^4$ and

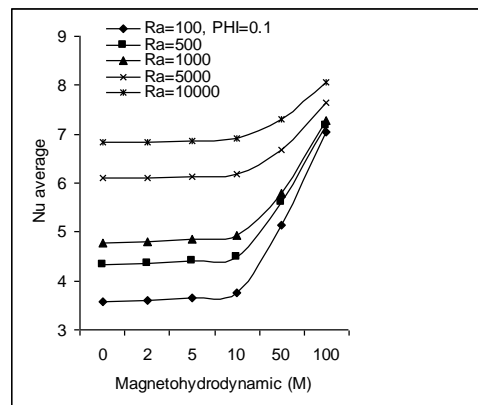


Fig. (11)Variation of average Nusselt number with magnetohydrodynamic for $\phi=0.1$ and for different Rayleigh number